

Waveguide-type optical passive ring resonator gyro using phase modulation spectroscopy technique

Huilian Ma, Xulin Zhang, Zhonghe Jin, and Chun Ding

Zhejiang University, Department of Information Science & Electronic Engineering, Hangzhou 310027 China
E-mail: mahl@zju.edu.cn

Abstract. We report the first demonstration of silica waveguide optical passive ring resonator gyro (OPRG) based on the phase modulation spectroscopy technique. The ring resonator is composed of a 6-cm-long silica waveguide. Observed from the resonance curve, the free spectral range (FSR) of the resonator, the full width at half maximum (FWHM) of the resonance curve, the finesse (F) of the resonator, and the resonance depth are 3.4 GHz, 62 MHz, 54.8, and 70%, respectively. The detection sensitivity of this OPRG will be 7.3×10^{-5} rad/s. In the experiments, there is an acoustic-optical modulator (AOM) in each light loop. We lock the lasing frequency at the resonance frequency of the silica waveguide ring resonator for counterclockwise (CCW) lightwave; the frequency difference between the driving frequencies of the two AOMs is equivalent to the Sagnac frequency difference caused by gyro rotation. Thus, the gyro output is observed. © 2006 Society of Photo-Optical Instrumentation Engineers.

[DOI: 10.1117/1.2280645]

Subject terms: gyro; ring resonator; silica waveguide; phase modulation spectroscopy technology.

Paper 050997LRR received Dec. 21, 2005; revised manuscript received May 23, 2006; accepted for publication May 28, 2006; published online Aug. 25, 2006.

A small, robust, tactical-grade performance gyro is vital for the successful implementation of the smart weapons and surveillance apparatus. A waveguide-type optical passive ring resonator gyro (OPRG) is a promising candidate.^{1,2} The OPRG is a frequency-sensitive device. The gyro rotation is determined by the resonance frequency difference in the clockwise (CW) and counterclockwise (CCW) lightwaves due to the Sagnac effect.¹ Light circulating many turns in the ring resonator can build up the Sagnac effect. Thus, a short-length sensing loop is required. In this letter, the phase modulation (PM) spectroscopy technique is chosen to detect the gyro signal using LiNbO₃ phase modulators.³ In the PM spectroscopy technique, the modulating signal and feedback signal do not interact, moreover the LiNbO₃ phase modulators are easy to be integrated with other optical devices. They will make the OPRG compact. Figure 1 shows a schematic diagram of the experimental setup of the OPRG system. The resonator is composed of a 6-cm-long silica waveguide ring and a directional coupler (C4). The wavelength of the laser is 1550 nm and the diameter of the resonator is 1.9 cm, so the scale-factor of the OPRG is¹ 0.84×10^4 Hz/rad s⁻¹.

The silica planar lightwave circuit (PLC) is the key rotating sensing element in the OPRG. It consists of two input/output directional couplers (C2 and C3) and one resonator coupler (C4). The coupling ratio of couplers C2 and C3 is designed as 50%. The coupling ratio of coupler C4 is optimized by the total loss in the ring resonator, including propagation loss of silica waveguide ring, excess loss due to the curvature, and excess loss through coupler C4. Considering the temporal coherence of the laser, the resonance curve of a ring resonator is given by^{4,5}

$$R = (1 - \alpha_c) \left[1 - \rho \frac{(1 - Q)^2}{(1 - Q)^2 + 4Q \sin^2(\delta/2)} \right], \quad (1)$$

where ρ is the resonance depth; δ is the phase shift around one trip of the ring; $Q = (1 - \alpha_R)^{1/2} (1 - k_C)^{1/2} (1 - \alpha_C)^{1/2} [\exp(-\pi \Delta f \tau)]$; α_R is the total propagation loss in the ring; k_C and α_C are the coupling ratio and coupling loss of resonator coupler C4, respectively; Δf is the spectral linewidth of the laser; and τ is the optical transmission time in the ring as nL/c . Here n is the refractive index of the silica waveguide, L is the ring length, and c is the velocity of the light in the vacuum. Gyro sensitivity is maximized when the slope of resonance dip is the largest; namely, when the total loss in the ring resonator and the linewidth of the laser are determined, there is an optimum k_C for gyro. Figure 2 shows the shot-noise-limited sensitivity and the finesse of the ring resonator versus the coupling ratio k_C . Here we use typical parameters of silica PLC and other devices. The losses of the waveguide and the coupler are assumed to be 0.01 dB/cm and 0.1 dB. The wavelength, spectral linewidth, and output power of the fiber laser are 1550 nm, 30 kHz, and 10 mW, respectively. The quantum efficiency of the photodiode (PD) is 0.8. The bandwidth of the measuring system is 1 Hz. The coupling ratio of coupler C4 is variable.

In the experiments, the resonance curve of the silica waveguide ring resonator was tested first. A low-frequency sawtooth waveform at 1 Hz was applied to the fiber laser, and then the frequency of the fiber laser changed linearly with time. The output of the ring resonator was monitored by a PD. The oscilloscope trace of Fig. 3 shows the applied voltage and the resonance curve observed in the PD. In Fig. 3, the applied voltage is a sawtooth wave with a voltage of about 20 V and a period of 1 s. For a deeper resonance curve, the times corresponding to the free spectral range (FSR) and the full width at half maximum (FWHM) are 680 ms and 12.4 ms, respectively. Because the frequency of the laser changes linearly with the input voltage at 250 MHz/V, the frequency of the fiber laser changes linearly with time at 5000 MHz/s. Thus, the FSR, FWHM, finesse (F), and the resonance depth of this ring resonator are 3.4 GHz, 62 MHz, 54.8, and 70%, respectively. The shallower resonance dips caused by the unadjusted eigenstate of polarization in the resonator can also be seen in the upper curve in Fig. 3. This may be overcome by using two polarization controllers (PCs) to adjust the polarization state of the input light before the silica PLC, as shown in Fig. 1.

The oscilloscope trace of Fig. 4 shows the demodulation curves at the high frequency lock-in amplifiers (LIAs) for both CW and CCW lightwaves. The separation between

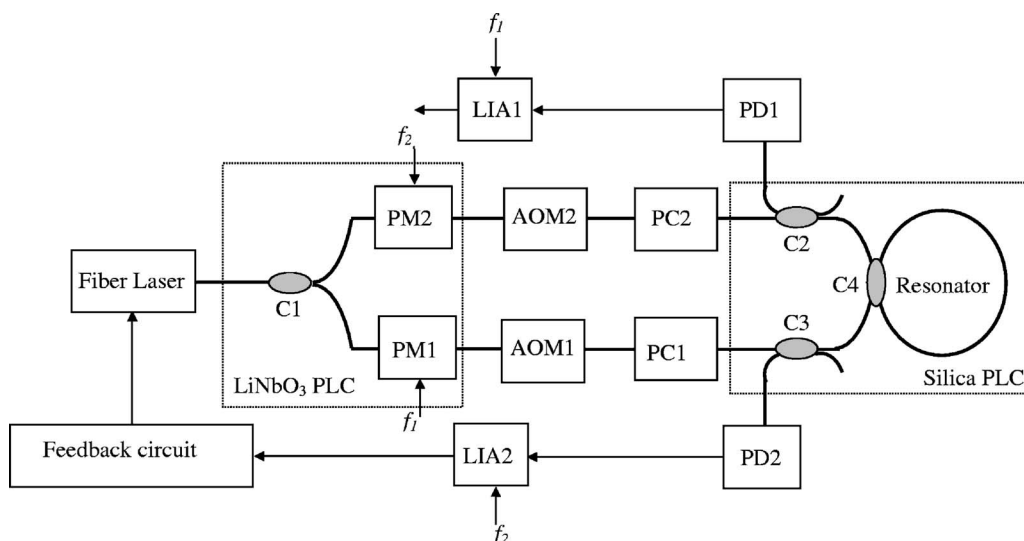


Fig. 1 Experimental setup of the OPRG using the PM spectroscopy technique.

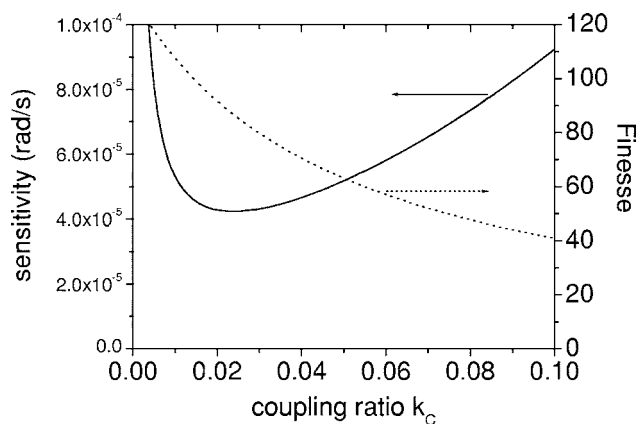


Fig. 2 Sensitivity and finesse versus coupling ratio k_c .

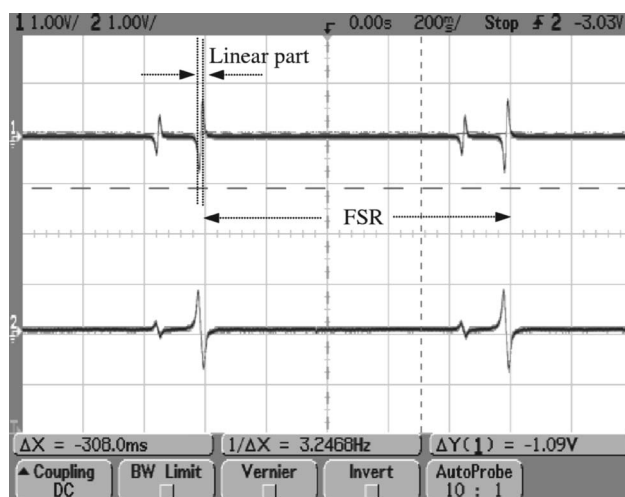


Fig. 4 Demodulation curves in CW and CCW directions.

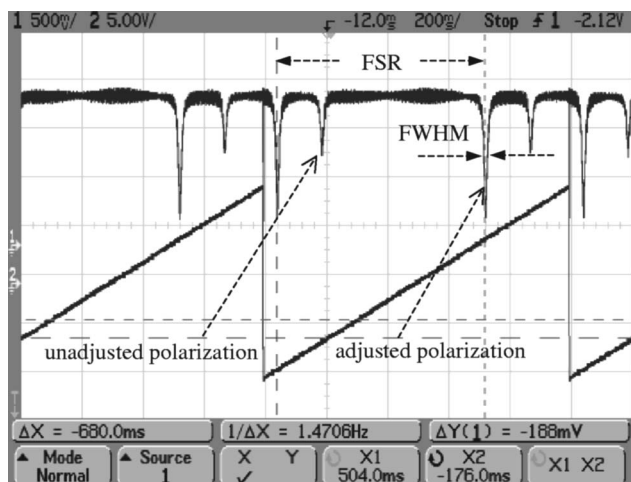


Fig. 3 Resonance curve of the fabricated silica PLC ring resonator.

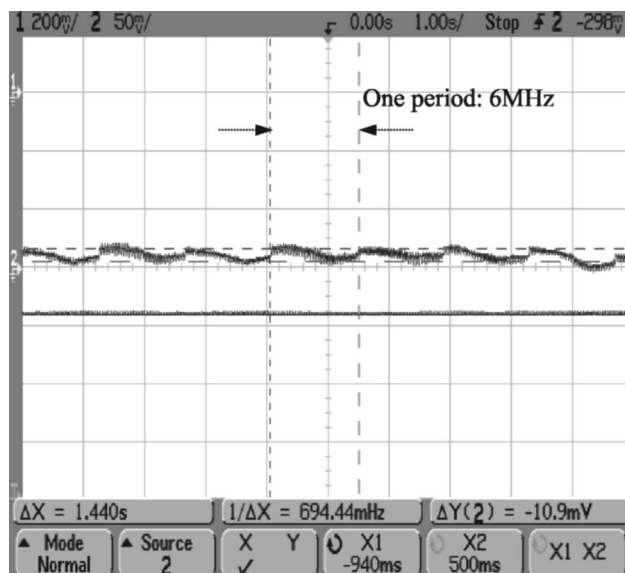


Fig. 5 Rotation observation with equivalent rotation input.

each discriminant is the FSR. From Fig. 4, we notice that the demodulation curve has good linearity near the resonance point. The times corresponding to the linear part of the main resonance demodulation curve and one FSR are 26.7 ms and 1 s, respectively. This means that the frequency deviation Δf of the linear part is 90.78 MHz. The demodulation amplitude is 1.62 V. Thus, the slope of the demodulation curve for linear part is 18 nV/Hz, since the scale factor of this OPRG is 0.84×10^4 Hz/rad s⁻¹. Considering the present level of the low noise detection circuit, a signal larger than 11 nV can be measured.⁶ Thus, the detection sensitivity of this OPRG will be 7.3×10^{-5} rad/s. The discriminant corresponding to the shallower dips, as shown in Fig. 4, is also demodulated clearly. This verifies that the designed high-frequency LIA has high demodulation accuracy.

After having obtained the parameters of the resonator, the open-loop system was set up. The acousto-optical modulator AOM1 (AOM2) between the PM1 (PM2) and C1 (C2) is used to give additional frequency shift for the CW (CCW) lightwave. When the fiber laser frequency f_0 is locked to the resonance frequency f_{CCW} in the CCW lightwave by the feedback circuit, the PD output in the CCW lightwave is stable, as shown in the lower curve in Fig. 5. The difference between the driving frequencies of the two AOMs is equivalent to the Sagnac frequency difference due to gyro rotation. The driving frequency of AOM2 is 40 MHz, while the driving frequency of AOM1 changes linearly with time from 43 to 37 MHz. Thus, the equivalent Sagnac frequency difference between CCW and CW lightwaves will also change from 3 to -3 MHz linearly with

time. The equivalent gyro output is shown in the upper curve in Fig. 5. As seen from Fig. 5, the gyro output corresponding to a 6-MHz frequency difference is 10.9 mV. It is close to the calculated results 10.8 mV from Fig. 4.

In this letter, an open-loop-operation OPRG based on the phase modulation spectroscopy technique was setup. The resonator parameters were measured and the detection sensitivity of this OPRG will be 7.3×10^{-5} rad/s. Additionally, the gyro output was observed with equivalent rotation input.

Acknowledgments

The authors would like to acknowledge the Excellent Young Teachers Program of MOE, China, for their support (2003 No. 355).

References

1. S. Ezekiel and R. Balsamo, "Passive ring resonator gyroscope," *Appl. Phys. Lett.* **30**(9), 478–480 (1977).
2. K. Suzuki, K. Takiguchi, and K. Hotate, "Monolithically integrated resonator microoptic gyro on silica planar lightwave circuit," *J. Lightwave Technol.* **18**(1), 66–72 (2000).
3. X. Zhang, H. Ma, C. Ding, and Z. Jin, "Analysis on phase modulation spectroscopy of resonator fiber optic gyro," *Chin. J. Lasers* **32**(11), 1529–1533 (2005).
4. H. Ma, Z. Jin, C. Ding, and Y. Wang, "Influence of spectral linewidth of laser on resonance characteristics in fiber ring resonator," *Chin. J. Lasers* **30**(8), 731–734 (2003).
5. H. Ma, Z. Jin, C. Ding, and Y. Wang, "Research on signal detection method of resonator fiber optical gyro," *Chin. J. Lasers* **31**(8), 1001–1005 (2004).
6. G. Yang, H. Ma, X. Zhang, K. Zhou, and Z. Jin, "Design of high frequency lock-in amplifier applied in R-MOG," *Chin. J. Sens. Actuat.* **18**(4), 863–866 (2005).